**Published as:** MAPOSSA, A. B., SIBANDA, M. M., SITOE, A., FOCKE, W. W., BRAACK, L., NDONYANE, C., MOUATCHO, J., SMART, J., MUAIMBO, H., ANDROSCH, R. & LOOTS, M. T. 2019. Microporous polyolefin strands as controlled-release devices for mosquito repellents. *Chemical Engineering Journal,* 360, 435-44**4.**

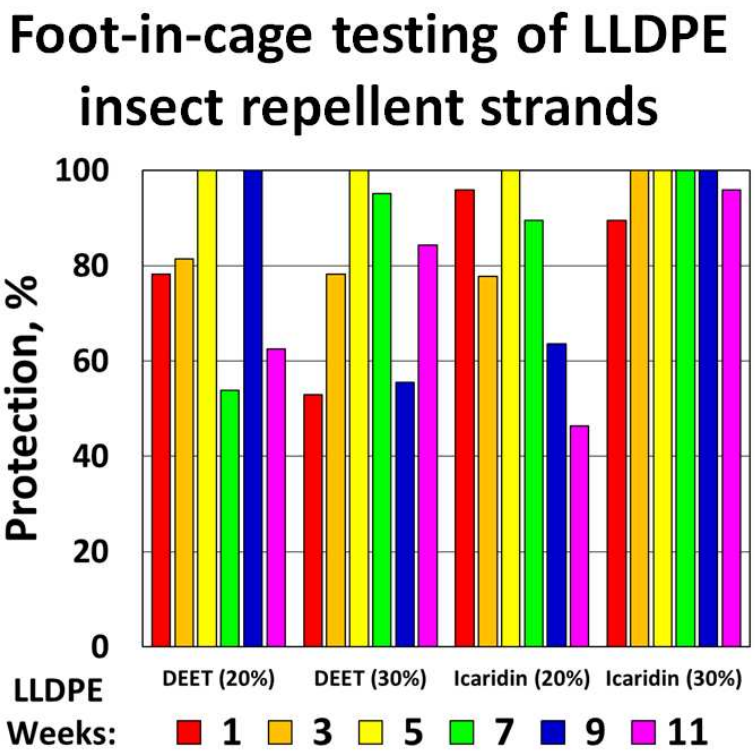

# Microporous polyolefin strands as controlled-release devices for mosquito repellents

António B. Mapossa,[a,b] Mthokozisi M. Sibanda,[a,b] Alcides Sitoe,[a,b] Walter W. Focke,[a,b,*] Leo Braack,[b] Cyril Ndonyane,[b] Joel Mouatcho,[b] Jansie Smart,[a] Herminio Muaimbo,[c] René Androsch[d] and Mattheüs Theodor Loots[e]

[a]Institute of Applied Materials, Department of Chemical Engineering, University of Pretoria, Lynnwood Road, Pretoria, South Africa. E-mail: walter.focke@up.ac.za

[b]UP Institute for Sustainable Malaria Control & MRC Collaborating Centre for Malaria Research, University of Pretoria, Private Bag X20, Hatfield 0028, Pretoria, South Africa, Pretoria, South Africa. E-mail: leo.braack@up.ac.za

[c]Department of Chemistry, Eduardo Mondlane University, Maputo, Mozambique. E-mail: hmuiambo.mz@gmail.com

[d]Interdisciplinary Center for Transfer-oriented Research in Natural Sciences, Martin Luther University Halle-Wittenberg, D-06099 Halle/ Saale, Germany. E-mail: rene.androsch@iw.uni-halle.de

[e]Department of Statistics, University of Pretoria, Private Bag X20, Hatfield 0028, South Africa. E-mail: theodor.loots@up.ac.za

## ABSTRACT

The main vectors of malaria in Africa, i.e. *An. arabiensis*, *An. gambiae s.s.* and *An. funestus*, are attracted by human foot odour and they tend to bite victims in the ankle area. Hence affordable mosquito-repellent polymer-foot bracelets with long lasting protection could reduce infective lower limb bites and therefore help to reduce the overall malaria transmission rate. This study investigated the possibility of increasing the duration of repellence activity by incorporating repellents into inexpensive thermoplastic polymers, namely poly(ethylene-co-vinyl acetate) (EVA) and linear low density polyethylene (LLDPE). Volatile repellents need to be released into the surrounding air to be effective, i.e. they are continuously lost to the atmosphere. This means that the bracelet should also act as a reservoir for relatively large quantities of the active compound. Towards this goal, polymer strands containing mosquito repellent were prepared by twin-screw extrusion compounding. A co-continuous phase structure was achieved by rapid quenching in an ice bath of the

homogeneous polymer-repellent melt exiting the extruder. Phase separation occurred through spinodal decomposition which trapped the liquid repellent in the microporous polymer matrix. The extruded polymer strands showed skin-like membranes that controlled the release rate. Strands that contained up to 30 wt-% of either DEET or Icaridin provided effective protection against mosquito bites even after 12 weeks of ageing at 50 °C.

**Keywords:** Mosquito repellent; controlled release; spinodal decomposition; DEET; Icaridin

## 1. Introduction

Malaria is a deadly disease with a large proportion of the world population at risk of infection. The annual number of malaria cases significantly exceeds 200 million and results in upwards of 400,000 deaths each year. Typically 90 % of these occur in Africa with approximately 74 % of them children under the age of 5 years [1]. The World Health Organization (WHO) is targeting elimination of malaria. For this to be achieved, the transmission of the malaria parasite from one person to the next by female *Anopheles* mosquito vectors must be prevented or at least significantly reduced [2]. This may be done by preventing or reducing the frequency of infective mosquito bites.

The continued prevalence of malaria in endemic areas is partly due to insufficient vector control measures. Long life insecticide treated nets (LLINs) and indoor residual spray (IRS) are the flagship interventions recommended by the WHO. The implementation of these vector control interventions has been met with significant success in reducing malaria transmission. However, LLIN and IRS only protect against indoor biting and resting mosquitoes. It is still possible for people to be infected with malaria whilst outdoors.

Judicious use of repellents might help prevent, or at least reduce, outdoor malaria transmission. Repellents are typically applied to exposed skin via topical formulations such

as lotions, sprays, emulsions, etc. N,N-diethyl-3-methylbenzamide (DEET) is a popular topical repellent in widespread use. It is applied to the skin at high concentrations (10–70 %) and has a residual effectiveness of a few hours [3, 4]. This short residual effectiveness necessitates repeated application in order to maintain constant repellent activity. This makes the use of topical repellents expensive particularly for resource-limited African communities where malaria is mostly prevalent. Slow and controlled release at effective levels may render the repellent long lasting [5-9].

Three of the main vectors of malaria in Africa (*An. arabiensis, An. gambiae s.s. and An. funestus*) are attracted by human foot odour, a smell similar to limburger cheese, and they tend to bite victims in the ankle area [10-12]. These vectors prefer feeding close to the ground level, i.e., at lower leg, ankles and feet [12, 13]. It has been shown that if these areas are protected, then vector mosquitoes do not move higher up the body to seek alternate biting areas, leading to a reduction in biting intensity [13]. Hence a long-life mosquito repellent polymer-foot bracelet could reduce infective lower limb bites by these vectors and therefore help to reduce the overall malaria transmission rates especially under outdoor conditions.

Malaria is highly endemic in the poorer regions of Africa [1]. Consequently two objectives have to be met when considering such vector control interventions. They should be highly affordable and should provide long lasting protection. Polymer-based carrier systems for insect repellent delivery were recently reviewed [14]. This study investigated the possibility of increasing the duration of repellence activity by incorporating repellents into thermoplastic polymers, namely poly(ethylene-co-vinyl acetate) (EVA) and linear low density polyethylene (LLDPE). If feasible, it could allow cost-effective bracelet manufacture via a conventional plastics extrusion processes. The objective is to develop systems with long-lasting efficacy, i.e., slow release of the active ingredient over an extended period of

time. In this way it may be possible to protect people against malaria infection during the time they spend outdoors.

The mechanism of slow release from polymers varies. When an additive is added to a polymer at levels that exceeds its solubility limit it will form a separate phase or bleed to the surface of the polymer. This so-called “blooming” is desirable for contact poisons as the active accumulates at the polymer surface. In fact, LLINs rely on this phenomenon of active blooming of the incorporated insecticides [15]. The insecticide needs to migrate to the surface and be retained there in order to be effective. Compared to solids, liquid additives migrate more rapidly out of a polymer matrix. They are also removed more easily by washing [15]. Liquid repellents also tend to be more volatile than solid insecticides used in the manufacture of LLINs. In contrast to the contact insecticides, repellents need to be released into the surrounding air to be effective. This means that in the case of the repellents, comparatively higher loadings are required than for insecticides since they are continuously lost to the surroundings. It is therefore unlikely that polymer-based liquid repellent-release systems will be able to maintain efficacy for very long times (e.g. more than one year) achieved with LLINs. However, premature loss of efficacy of repellent-containing bracelets must be avoided. Fortunately the insights and experience gained during the study of LLINs can help to guide the development of long lasting repellent bracelets.

Consider the situation in which the active ingredient dissolves in the polymer matrix. Since repellents are liquid at ambient conditions, the polymer matrix must be chosen carefully to maximise the range of thermodynamic miscibility. The solubility limit cannot be exceeded as this may result in an oily film forming at the surface of the bracelet which may cause discomfort to the user. Since the repellent is released continuously into the surrounding atmosphere as soon as it reaches the polymer surface, the active loading must be high to

maintain activity over an extended period of time. This implies that large quantities of the active should be available and this requires a significant solubility in the polymer matrix.

Unfortunately using a polymer matrix in which the active is dissolved has drawbacks too. Firstly, the solubility of an active in a polymer matrix may be limited. This is due to the fact that the driving force for miscibility, the Gibbs energy of mixing, is low when polymers are involved. On the other hand, high solubility implies extensive swelling of the polymer. This leads to dimensional stability issues, e.g., extensive shrinking as the active is depleted over time.

The alternative concept proposed herewith utilises porous polymer strands for this purpose. The internal open-cell polymer foam structure serves both as a reservoir and a protective environment for the active ingredient trapped inside. Ideally, an outer dense skin layer should provide the diffusion barrier that controls the release of repellent at effective levels over a considerable period of time.

Microporous polymer matrices may provide a solution to these problems. In this case the insoluble or only partially soluble active liquid is trapped in the open pores of the polymer matrix. Such a system can be generated directly via an extrusion process that facilitates the formation of a co-continuous phase structure comprising polymer-rich and repellent-rich domains. This can be achieved through the phase separation phenomenon of spinodal decomposition provided the repellent and the polymer melt form a homogeneous solution at high temperatures. This type of phase separation occurs when such a mixture is rapidly cooled to a temperature in the spinodal region of the phase diagram [16-20]. Besides the crystallization-induced solid-liquid phase separation technique which recently has been applied to entrap DEET in poly(lactic acid) [21, 22], spinodal-decomposition based liquid-liquid phase separation is widely used in the manufacture of porous membranes. A typical phase diagram showing the phase behaviour of a polymer-liquid repellent combination is

shown in Figure 1 [23]. The system exhibits an upper critical solution temperature ($T_{UC}$) and features a stable single-phase region together with a metastable and an unstable region.

In polymer-repellent mixtures the loci of the phase boundaries can be described by the Flory-Huggins theory [24]. At temperatures above the upper critical solution temperature, the system is fully miscible for all compositions. Below this temperature, phase separation can occur at a temperature which depends on the concentration of the system components. The compositions of the two phases in equilibrium at any temperature are defined by the binodal line. In the meta-stable region indicated in the phase diagram, the phase separation will occur via a nucleation and growth mechanism. This is the usual scenario for liquid-liquid phase separation. If the polymer represents the minority phase, it may initially lead to the undesirable formation of separate polymer particles that are suspended in the continuous liquid repellent phase.

Inside the two-phase region there is another set of phase envelopes, the spinodal curves. In this region of the phase diagram a homogeneous mixture is thermodynamically completely unstable. In contrast to the metastable bimodal region, the solution will spontaneously split into two phases via spinodal decomposition, a polymer-rich phase and a solvent-rich phase. Phase separation by this mechanism leads to a finely dispersed microstructure via diffusion processes that amplify intrinsic thermodynamic spatial composition fluctuations. Ultimately this co-continuous structure may be fixed by either the subsequent crystallization of the polymer, or by vitrification of the polymer-rich phase. This means that the majority liquid phase is trapped inside a solid polymer-rich phase (which still may contain a minor amount of repellent) with a porous structure. In practice such microporous microstructures are often achieved by rapid quenching of a homogeneous melt in a cold water bath.

It is important to note that the emphasis of this communication is to report on the conceptual development of a suitable carrier material for incorporation of repellent substances and subsequent stable release of the repellent over an extended period. The paper therefore emphasizes the physical and chemical elements and basic entomological impact. With proof-of-concept achieved, it will be possible to refine the microporous polyolefin strands into various products for field application to reduce malaria transmission, such as by way of anklets, footlets, or bracelets. More extensive and rigorous entomological and epidemiological testing will be required on more refined products before they could become commercially acceptable.

<Insert Figure 1>

## 2. Materials and methods

### *2.1. Materials*

The insect repellent N,N-diethyl-3-methylbenzamide (DEET) [CAS No. 134-62-3] was obtained from Sigma-Aldrich. It had a purity of ≥ 97% and a density of 0.998 g $cm^{-3}$ at 20 °C. 1-(1-methylpropoxycarbonyl)-2-(2-hydroxyethyl)piperidine (Icaridin) [CAS No. 119515-38-7] was supplied by Saltigo under the trade name Saltidin®. According to the supplier the purity exceeded 97%, the boiling point is 272 °C and the density is 1.0362 g $cm^{-3}$ at 20 °C. Dichloromethane [CAS No. 75-09-2] of purity is 99.9% was obtained from Merck.

Poly(ethylene-co-vinyl acetate) (EVA) (grade Elvax 760A ex DuPont) pellets were pulverised by Dreamweaver. The VA content was 9 %, the density 0.930 g $cm^{-3}$ and the melt flow index (MFI) 2.0 g/10 min (190 °C/2.16 kg). Linear low density polyethylene (LLDPE)

(Sasol HR411) was obtained from Sasol. The density was 0.939 g $cm^{-3}$ and MFI was 3.5 g/10 min (190 °C/2.16 kg).

Dellite 43B organo-modified clay was supplied by Laviosa Chimica Mineraria S.p.A. The approximate medium particle size was 8 μm. This organoclay, intercalated with dimethyl benzyl hydrogenated tallow ammonium, was used to modify the rheological consistency of the liquid repellents.

*2.2. Extrusion compounding*

The organoclay was included in all the formulations to partially "solidify" the liquid repellent in order to assist feeding of the mixture via the hopper of the compounding extruder and to facilitate good mixing and rapid dissolution in the polymer melt. The extrusion-compounding of all the EVA and LLDPE compositions was performed on a TX28P 28 mm co-rotating twin-screw laboratory extruder with a screw diameter of 28 mm and an L/D ratio of 18. The screw design of this machine comprised intermeshing kneader blocks that also imparted a forward transport action.

Polymer-clay nanocomposites were prepared by first dispersing the clay into the polymer powder with a Sigma spice grinder. The powder blends were then compounded on the TX28P 28 mm co-rotating twin-screw extruder. The extruded strands were cooled by passing them through a water bath. The strands were granulated on a Chen Shin Machinery Co., Ltd, Model CT-300 pelletizer.

Strands containing the liquid repellents were produced in a similar manner except that they were not pelletized. The polymer and clay powders were first mixed together in a plastic container to obtain a semi-dry consistence that could be fed into the compounding extruder. The temperature profiles, from hopper to die, were set at 140 /160 /160 /160 °C and 140 /160 /170 /170 °C for EVA and LLDPE compositions respectively. The screw speed was varied

from 105 to 150 rpm. The exiting polymer strands were quench-cooled in an ice-water bath. LLDPE strands with diameters ranging from 2.5 to 5.1 mm were obtained while for EVA strands the diameters ranged from 3.2 to 6.4 mm. The diameters of polymers strands were measured with a Mitutoyo Digital Calliper with a measurement range up to 150 mm.

The films used for permeability measurements were blown using a Collin BL 180/400 blown film unit. It comprised a 30 mm diameter single screw extruder with L/D = 25. The blown film die had a diameter of 60 mm and featured a dual-lip cooling ring. The extruder was operated at a screw speed of 40 rpm. The temperature profiles, from hopper to die, were 170/190/190/190/190/190/190/190 °C and 190/200/205/205/205/205/205/195 °C for EVA and LLDPE nanocomposite films respectively. The final film thicknesses were measured with a Mitutoyo Digital micrometer with a resolution of 1 μm. The reported film thicknesses represent the average of five separate measurements.

*2.3. Absorption of repellent by the polymers*

Approximately 4 g of neat EVA and LLDPE pellets were weighed and placed in Polytop glass vials containing approximately 16 mL DEET or Icaridin. The vials were placed in either an EcoTherm-Labcon or a Scientific Series 9000 forced convection oven, set at a temperature of 50 °C. After three days, the pellets were removed, and the excess repellent was removed using a quick rinse with dichloromethane. The repellent absorption was estimated from the recorded mass gain of the pellets.

*2.4. Polymer film permeability test***s**

The permeability of the blown films were determined using Payne permeability cups. The internal diameter of the cups was 54.9 mm and they had a depth of 19.7 mm. They were partially filled with mosquito repellent before clamping the polymer films in place. The cups

were placed in convection ovens set at a temperature of 50 ºC. The mass loss was measured daily over a period of two weeks. The permeability was estimated from the slope of the linear mass loss when plotted as a function of time.

*2.5. Repellent content by solvent extraction and thermogravimeric analysis (TGA)*

Polymer strands containing repellents and approximately 70 mm long were cut, weighed and placed in Polytop glass vials. Approximately 40 mL dichloromethane was added and the vials stoppered. The extraction solvent was replaced on a daily basis. After the fifth extraction, the strands were removed and allowed to dry in a fume hood at ambient temperature. The repellent content was estimated from the recorded mass loss of the strands in the dried form. The repellent content of the polymer strands was also investigated using TGA on either a Hitachi STA-7300 or a TA Instruments SDT-Q600 Simultaneous TGA/DSC. Samples, weighing approximately 16 mg, were heated from ambient temperature to 600 °C at a rate of 10 K $min^{-1}$. The purge gas was nitrogen flowing at 50 mL $min^{-1}$. The first TGA mass-loss step of the polymer strand was associated with the loss of the repellent.

*2.6. Scanning electron microscopy*

Repellent-free polymer strands were immersed in liquid nitrogen for approximately 1 h and then fractured. The fracture surface was coated six times with carbon using an Emitech K950X sputter coater prior to analysis. The samples were viewed with a Zeiss Ultra 55 Field Emission Scanning Electron Microscope at acceleration voltages of 1 kV and 5 kV.

*2.7. Repellent release studie***s**

Daily maximum temperatures during peak malaria transmission periods in many areas of Africa often exceed 40 ºC and it was desired to test the product at high temperature

challenge. For this reason the time-dependent repellent release from the strands was determined by ageing at 50 °C in either a Scientific Series 9000 or an EcoTherm-Labcon forced convection oven. The strands were suspended from the inside roof of the ovens in the form of loose coils. They were weighed twice a week. Every two weeks, samples measuring 3.0 m in length, were removed for foot-in-cage bioassay tests as described below. The mass loss and repellence testing was done for up to 12 weeks.

*2.8. Repellent efficacy studies*

Ethical clearance for the repellence testing study was obtained from the Faculty of Health Sciences ethics committee of the University of Pretoria (Protocol No. 82/2016). The tests for mosquito repellent efficacy were conducted under controlled insectary conditions. Caged mosquitoes were offered dual-choice opportunity for feeding at treated/untreated body parts of human volunteers [25, 26]. In the case of the study reported on here, the insectary colony of *Anopheles arabiensis* was derived from stock material maintained by the South African National Institute for Communicable Diseases (NICD). Three hundred mixed-gender mosquitoes were placed in a large (1200 mm × 600 mm × 600 mm) netting cage which, on one side, had two entry portals for the insertion of legs, spaced ca. 500 mm apart. Every effort was made to ensure minimal disturbance of mosquitoes prior to each test, and no blood-meals were offered for 72 h prior to each trial to ensure that the female mosquitoes were starved and would readily try to bite and feed. All mosquitoes were kept and trials conducted within the insectary which is maintained at a constant temperature of 25 ± 2 °C and relative humidity of 75 ± 5 %. Mosquitoes did have access to cotton-wool soaked with a 10% sugar solution which was removed 6 h prior to commencement of repellent trials.

The experimental design was as follows: Strands were prepared compounded using two different polymers (EVA and LLDPE), containing two different repellents (DEET and

Icaridin) at two different levels (20 and 30 wt-%). The repellence tests were done on three different individuals with different blood groups (A, B and O, all three $Rh^+$).

The test strand, 3.0 m long, was wound around the lower limb region of one leg of a volunteer (Figure 2), leaving the other leg fully exposed. No socks or shoes or any other item of clothing was worn below the knee. Both legs were then inserted into the cage, one leg per entry hole, and the person would stand still for five minutes. At the end of the five minutes two other persons would use flashlights to count the number of mosquitos present on each of the lower legs of the test person. The number of mosquitoes on the treated and untreated legs was recorded separately. Although in most cases it was possible to feel or see which mosquitoes were feeding, no distinction was made between feeding or resting mosquitoes, in accordance with standard WHO protocol [27]. As long as the mosquito was stationary on the foot or lower leg for at least five seconds it was counted. Only mosquitoes below the mid-calf region were counted (halfway between foot and knee). To avoid possible build-up of repellent on any one ankle due to continuous use, each person would use the alternate ankle on every alternative test day. Tests were conducted at least three days apart, starting at 15h00, allowing sufficient time for mosquitoes not to become accustomed to any odour which may linger after each application.

The degree of protection ($p$) was calculated as the proportion of the number of mosquito-landing and/or probing on the treated leg ($N_T$) in relation to the number of landing and/or probing on the control leg ($N_C$) of the same individual [28, 29]:

$$p = (N_C - N_T) / (N_C + N_T)$$

The degree of protection is reported in percentage units.

<Insert Figure 2>

## 3. Modelling the repellent release from strands

Figure 3 shows a schematic of a long cylindrical microporous strand covered by a thin membrane-like outer skin layer, serving as a model for discussion of the repellent-release characteristics. The geometric features of this model were informed by the SEM results presented below. The cross-section is circular and the structure of the inner polymer section was assumed microporous. Conceptually it corresponds to an open-cell polymer foam that is initially completely filled with the liquid repellent. As the repellent is gradually released to the atmosphere, it is assumed that the outer pores are progressively emptied and the lost liquid is replaced by air and repellent vapour. To a first approximation, it is assumed that the location of the liquid-vapour boundary is concentric with the outer wall.

<Insert Figure 3>

In order for the active compound to be released from the strand, a portion of the liquid evaporates and diffuses through the porous matrix towards the outer membrane. The matrix polymer forms both the microporous structure and the outer membrane. The permeability of the repellent through this membrane is defined by the product of its solubility in the membrane and the diffusion coefficient inside the membrane. The implication is that the active is also dissolved in the rests of the microporous polymer structure. This has several implications including the fact that the polymer structure could change shape (e.g. shrink) and that it can contribute to the rate of mass transport. However, in this first-cut analysis these effects are ignored. The fact that the active must diffuse through a porous polymer maze also affects the release rate. Therefore it is necessary to consider the transport mechanisms of the active ingredient in the porous region in addition to the permeation through the membrane. In reality surface tension will affect the shape of the liquid meniscus inside

partially filled pores. This has implications for the rate at which the liquid transforms into vapour, i.e. the evaporation rate. This is not taken into account presently. Finally, it is assumed that, once the repellent molecules reach the outside surface of the strand, they are so rapidly removed by convection air currents so that it can be assumed that the concentration on the outside surface of the strand is negligible.

The mathematical model for the release of the repellent assumes that it is determined by vapour diffusion in the porous regions and by permeation through the outer skin layer. At the inner liquid surface the repellent evaporates into the porous region. It then diffuses via the air-filled pores towards the membrane where it dissolves in the polymer and permeates to the outside. The assumptions forming the basis of the model can be summarised as follows.

- The porosity of the microporous region is $\varepsilon$
- The liquid-filled region is located concentric to the main polymer cylindrical polymer strand
- The diffusion equation holds for both the porous region as well as for the membrane but the effective diffusion coefficients differ
- The equilibrium vapour concentration at the liquid interface can be estimated from the ideal gas expression $\rho_{eq} = M_A P_A^{sat} / RT$ which expresses the equilibrium mass density ($\rho_{eq}$) of the repellent at the temperature $T$ in Kelvin in terms of its molar mass ($M_A$) and its vapour pressure ($P_A^{sat}$) with $R$ denoting the gas constant.
- The solubility of the repellent in the membrane is described by Henry's law
- The evaporation rate is very slow so that quasi-steady state diffusion may be assumed.

The initial mass of repellent inside a strand, for which the diameter of the porous region is $R_P$, is $m_o = \rho_L \varepsilon \pi R_P^2 L$. After some time, during which part of the repellent has evaporated,

the fraction repellent remaining will be equal to $X = m(t)/m_o$ and the remaining liquid is assumed to be confined to a co-axial cylindrical body with radius $R_L$. The total amount of the repellent remaining in a filament of length $L$ is given by Equation (1):

$$X(t) = \frac{2}{R_P^2 C_L}\int_{R_L}^{R_P} r\,C(r,t)\,dr + \left(\frac{R_L}{R_P}\right)^2 \tag{1}$$

However, the first term is negligible compared to the second term because, compared to the liquid, the repellent vapour density is very low. So it may be assumed that

$$X(t) \approx \left(R_L/R_P\right)^2 \tag{2}$$

The governing diffusion equation reads as follows:

$$\frac{\partial \rho}{\partial t} = \frac{D_{eff}}{r}\left(\frac{\partial}{\partial r}\left(r\frac{\partial \rho}{\partial r}\right)\right) \tag{3}$$

This equation holds for both the outer membrane and the vapour-filled porous region but the effective diffusion coefficients in these two regions are assumed to be different. The initial and boundary conditions are:

$$\begin{array}{lll} t = 0 & 0 < r < R_p & \rho = \rho_L \\ t > 0 & r = R_L & \rho = \rho_{eq} \\ & r = R_P & \rho_M(R_P^+) = H\,\rho_P(R_P^-) \\ & & D_P \dfrac{\partial \rho}{\partial r}\Big)_{r=R_P^-} = D_M \dfrac{\partial \rho}{\partial r}\Big)_{r=R_P^+} \\ & r = R_F & \rho = 0 \end{array} \tag{4}$$

The assumption of quasi-steady state conditions is justified by the fact that the release rate is very low. This reduces the problem to solving the following differential equation:

$$\frac{d}{dr}\left(r\frac{d\rho}{dr}\right) = 0 \tag{5}$$

The solution of equation (5), subject to the initial and boundary conditions in (4), yields expressions for the concentration profiles in the membrane and the microporous regions for a

given value of the stationary liquid core radius $R_L$. The rate at which the repellent evaporates is related to the rate at which $R_L$ decreases:

$$\rho_L \frac{dR_L}{dt} = D_P \frac{\partial \rho}{\partial r}\Big)_{r=R_L^+} \tag{6}$$

Analysis, taking this into expression into account, yields an implicit expression that links the amount of repellent released ($X$) to the elapsed time ($t$):

$$\kappa_1 t = \kappa_2 \left(1 - X\right) + X\,\ell n\, X \tag{7}$$

where $$\kappa_1 = \frac{4D_P}{R_P^2}\frac{\rho_{eq}}{\rho_L} \text{ and } \kappa_2 = \left[1 + \frac{\alpha}{H}\ell n\left(\frac{R_F}{R_P}\right)^2\right] \tag{8}$$

The model provides an approximate expression for the repellent content of the strand for the situation where both the membrane and the porous region influence the rate of release.

Note that $\kappa_2 = 1$ in the complete absence of a rate controlling membrane layer. Alternatively, when the outer skin-like membrane fully controls the repellent release the model defined by equation (7), simplifies to a simpler expression:

$$\kappa_3 t = 1 - X \tag{9}$$

With $$\kappa_3 = \frac{2HD_M}{R_P^2 \ell n\left(R_F/R_P\right)}\left(\frac{\rho_{eq}}{\rho_L}\right) \tag{10}$$

This expression also holds at the beginning of the repellent release when the porous regions of the strand are still completely filled with liquid. The rate of repellent mass release from a strand, of length $L$, for which the membrane is rate controlling, is:

$$J \approx -\varepsilon\rho_L \pi R_F^2 L\frac{dX}{dt} = \frac{2\varepsilon\rho_{eq}\pi L D_M H}{\ell n\left(R_F/R_P\right)}\left(\frac{R_F}{R_P}\right)^2 \tag{11}$$

In the more general case the corresponding expression is:

$$J = 4\varepsilon\rho_{eq}\pi L D_P H (R_F/R_P)^2 \Big/ \ell n\left[X^{-H}\left(R_F/R_P\right)^{2\alpha}\right] \tag{12}$$

## 4. Results and discussion

### *4.1. Polymer swelling and film permeability*

Ageing of the microporous repellent-filled strands were conducted at 50 °C. This represents an upper limit to the ambient temperatures that may be experienced in malaria-endemic regions. Selecting this temperature also reduces the required experimental time as evaporation is expected to be faster at elevated temperatures. Consequently, in order to obtain relevant physical data, the repellent absorption and permeability tests were also conducted at 50 °C.

Table 1 lists the amount of repellent absorbed by the two polymers at 50 °C and also the permeability of films containing 5 wt-% Dellite 43B organoclay. As expected, less of the polar repellents was absorbed by the highly nonpolar and semicrystalline LLDPE compared to the more polar EVA matrix of lower crystallinity than LLDPE. However, the permeability values for the corresponding films were similar in magnitude. Both the solubility and the permeability values for Icaridin were about half of those measured for DEET. Icaridin is also less volatile and this raises the expectation that, all other conditions being equal, that the release of this repellent will be slower than that for DEET.

### *4.2. Repellent content of the extruded strands*

Figure 4 shows representative TGA results, obtained in a nitrogen atmosphere, for the repellent, the neat polymer and repellent-filled polymer strands. Evaporative mass loss of the neat DEET commenced just above 105 °C and was complete by 268 °C. The loss of DEET from the LLDPE is slightly delayed by the fact that it was trapped inside the pores of the microporous polymer matrix. However, the DEET mass loss is complete before the LLDPE starts to lose mass in earnest above 400 °C.

Similar trends are observed for the DEET-filled EVA except that the DEET mass loss by evaporation overlaps with the first mass-loss event for the polymer. The DEET evaporation from the EVA matrix appears significantly impeded. This is tentatively attributed to differences in the microstructure of the DEET porosity and the DEET being partially soluble in the EVA at these very high temperatures.

<Insert Table 1>

<Insert Table 2>

<Insert Figure 4>

Table 2 lists sample compositions together with the relevant repellent contents as determined by solvent extraction mass loss studies. The extraction results corresponded well to the amount of repellent added in the compounding step showing that very little repellent was lost during processing.

*4.3. Scanning electron microscopy*

Figures 5 shows the effect of the repellent type and its concentration on the LLDPE phase morphology as made visible by solvent extraction. The observed microporous nature is consistent with the expected co-continuous structure expected when the phase separation occurs via spinodal decomposition. However, it is clear from Figure 5 that the nature of the repellent, as well as the concentration that was used, did affect the final microstructure. Interestingly, no clay platelets were observed suggesting that they were confined to the polymer-rich phase that formed the microporous scaffold. Similar observations were made for LLDPE compositions containing Icaridin as repellent. The EVA-repellent combinations

showed finer, more complex microstructures and these will be reported in a separate communication.

<Insert Figure 5>

<Insert Figure 6>

Figure 6 compares the outer surface with the inner structure of an LLDPE strand initially filled with DEET. The pronounced edge and the smooth outer surfaces seen in Figure 6 provide evidence for the presence of a denser membrane-like skin covering the microporous strands.

<Insert Figure 7>

*4.4. Repellent release studies*

Figure 7 shows measured repellent release curves for LLDPE and EVA strands aged in the convection oven set at a temperature of 50 °C. Figure 7(a) reveals that relative release of DEET, at similar concentrations, occurred faster from EVA strands compared to LLDPE strands. The situation is more complicated for the Icaridin-containing strands. In this case the fraction repellent released occurred fastest and slowest for the LLDPE strands containing 20 wt-% and 30 wt-% Icaridin respectively.

The solid lines in Figure 7 show trend lines based on equation (7). In all cases reasonable fits to the experimental data were obtained. The adjustable model parameters were determined by least square data fitting and they are listed in Table 2. In some cases the simpler expression, equation (9), provided adequate data fits and for those $\kappa_3$ values are also listed.

*4.5. Repellence testing*

Initial foot-in-cage experiments compared untreated feet with feet covered by neat EVA or LLDPE polymer strands. Surprisingly it was observed that the mosquitoes preferred probing the foot covered by repellent-free strands rather than the fully exposed foot. The degree of protection, averaged over both the neat LLDPE and EVA strands, was estimated at -19 ± 8 %. This means that the mosquitoes were actually attracted to feet covered by neat, repellent-free strands. The reasons for this behaviour is not currently understood. However, this result informed the decision to conduct all the foot-in-cage tests comparing a covered foot to a bare one rather than one covered by an inert strand.

Table 3 reports the results of the foot-in-cage tests. A statistical analysis of the results is presented in the Supplementary Material. First a parametric analysis of variance (ANOVA) was performed in order to detect significant factors that might have an influence on the protection measurements obtained for the repellents. Following this, a non-parametric ANOVA was performed using the Kruskal-Wallis test, which makes no assumptions of the underlying data structure. Under all these tests, the null hypothesis was that there are no effects observed. The important conclusions of the statistical analysis were that, at the 5 % level of confidence, neither polymer, repellent type, repellent level, test person, treated foot, nor ageing time had a significant effect on the level of protection provided. Although no significant effects could be detected between the different treatments, they all differed significantly from the untreated feet, indicating that being treated, differed significantly from not being treated, i.e. had significantly less mosquito probings. The implication is that all the strands provided similar level of protection against mosquito bites for up to 12 weeks.

The observation that oven ageing time did not have a statistically significant effect on the degree of protection was expected since the measured mass loss rate of the strands was

approximately constant over time. This implies that all the repellence tests conducted over the full oven ageing time for a given strand represent repeat measurements of its protection performance. Figure 8 shows such combined foot-in-cage repellent test results for each of the LLDPE- and EVA-based strands, all of which contained 5 wt-% Dellite 43B clay. The results presented in Figure 8 suggest that the best repellence performance was obtained with the LLDPE strands that initially contained 30 wt-% Icaridin.

<Insert Table 3>

<Insert Figure 8>

**5. Discussion**

The initial release rate of the repellents is determined by the resistance to permeation posed by the outer skin membrane. As the inner liquid becomes depleted, the tortuous nature of the microporous region imposes an additional resistance to repellent vapour transport and release. However, it is clear that for some of the strands the membrane remained the rate controlling barrier for repellent release. This was the case for the strands containing 30 wt-% DEET and the Icaridin-containing EVA strands. The initial repellent release data in combination with the permeability values measured for the blown films allowed the estimation of the effective thickness of the skin-like membranes covering the strands. These estimated values are listed in Table 2. They vary from 4 to 20 μm for DEET-containing strands and from 26 to 40 μm for the Icaridin-based strands. These values are in order of magnitude agreement with SEM observations as illustrated in Figure 6. The much thicker membrane coverings of the Icaridin-based strands, compared to the DEET-based strands, and the lower vapour pressure of the former repellent most likely explains the slower release observed in Figure 7(b). Despite the slower release, the Icaridin strands provided similar protection against mosquitoes biting in

the foot-in-cage tests used in this study. Excellent repellence was achieved for the duration of the repellence testing, i.e., for up to 12 weeks.

This results of this study suggest the possibility of developing long-life mosquito-repellent anklets/footlets/bracelets. However, more work will be required to understand the formation and thickness control of the membrane-like skin found on the surface of the extruded strands. It is possible that the trapping of the repellents inside the microporous structures of the strands also reduces direct skin contact. However, additional experimental exploration will be required to confirm this potential advantage.

## 6. Conclusions

Mosquito repelling polyolefin strands, containing significant quantities of mosquito repellents (20 or 30 wt-%) can be produced by an extrusion-compounding process. The rapid cooling induced by extruding the exiting strands directly into ice cold water bath facilitates phase separation of the repellent oil and the polymer via spinodal decomposition. This leads to an open-cell microporous polymer scaffold which traps the liquid repellent in the polymer matrix. The extrusion process also yields a thin integral skin that covers the extruded strands. To a large extent, this skin controls the release of the repellent at a low effective rate. The protection of such strands, wound around the foot and ankle area, were evaluated using a foot-in-cage mosquito repellence test. Strands that contained up to 30 wt-% of either DEET or Icaridin provided effective protection against mosquito bites up to 12 weeks of ageing in convection ovens set at a temperature of 50 °C. This suggests that they could be developed into cost-effective long-life mosquito repellent devices. Such long-lasting repellent products have the potential to play a highly significant role in disrupting malaria transmission under outdoor situations where malaria vectors have a strong preference for biting people on ankles and feet when in seated or standing position.

**Acknowledgements**

Financial support from the Deutsche Forschungsgemeinschaft (DFG) (Grant AN 212/22-1) is gratefully acknowledged. Mr Cyril Ndonyane is thanked for maintaining the *Anopheles* colony of the insectary. We also express our gratitude to him and Mr Robert Tewo for assisting with the repellent testing trials. Saltigo (Germany) is thanked for the generous gift of Saltidin® samples and Laviosa Chimica Mineraria S.p.A (Italy) for providing the Dellite 43B organoclay sample.

## References

[1] WHO, World Malaria Report 2015, in: WHO (Ed.), World Health Organisation, Switzerland, 2015.
[2] malERA, A Research Agenda for Malaria Eradication: Vector Control, PLoS medicine (2011).
[3] D. Ma, A.K. Bhattacharjee, R.K. Gupta, J.M. Karle, Predicting mosquito repellent potency of N,N-diethyl-m-toluamide (DEET) analogs from molecular electronic properties, American Journal of Tropical Medicine and Hygiene 60 (1999) 1-6.
[4] E. Lupi, C. Hatz, P. Schlagenhauf, The efficacy of repellents against Aedes, Anopheles, Culex and Ixodes spp. - A literature review, Travel Medicine and Infectious Disease 11 (2013) 374-411.
[5] R. N'Guessan, B.G.J. Knols, C. Pennetier, M. Rowland, DEET microencapsulation: a slow-release formulation enhancing the residual efficacy of bed nets against malaria vectors, Transactions of the Royal Society of Tropical Medicine and Hygiene 102 (2008) 259-262.
[6] J. Mokhtari, Nakedi, AS., and Sarli, MA., Synthesis and evaluation of a novel insect-repellent MCT reactive dye on Nylon 6, RMUTP International Conference: Textiles & Fashion 2012Bangkok, Thailand, 2012.
[7] J. Mokhtari, A. Shams-Nateri, P. Ferdosi, Synthesis and characterization of novel reactive dyes with simultaneous insect-repellent and anti-bacterial properties, Fibers and Polymers 15 (2014) 1369-1374.
[8] K. Ramya, V. Maheshwari, Development of eco friendly mosquito repellent fabric finished with andrographis paniculata plant extracts, International Journal of Pharmacy and Pharmaceutical Sciences 6 (2014) 115-117.
[9] T.T. Yao, L.K. Wang, J.L. Cheng, Y.Z. Hu, J.H. Zhao, G.N. Zhu, Optimization of pyrethroid and repellent on fabrics against Stegomyia albopicta (=Aedes albopictus) using a microencapsulation technique, Medical and Veterinary Entomology 29 (2015) 37-43.
[10] T. Dekker, W. Takken, B.G.J. Knols, E. Bouman, S. Van De Laak, A. De Bever, P.W.T. Huisman, Selection of biting sites on a human host by Anopheles gambiae s.s., An. arabiensis and An. quadriannulatus, Entomologia Experimentalis et Applicata 87 (1998) 295-300.
[11] B.G.J. Knols, R. De Jong, Limburger cheese as an attractant for the malaria mosquito Anopheles gambiae s.s, Parasitology Today 12 (1996) 159-161.

[12] L.E.O. Braack, M. Coetzee, R.H. Hunt, H. Biggs, A. Cornel, A. Gericke, Biting pattern and host-seeking behavior of Anopheles arabiensis (Diptera: Culicidae) in northeastern South Africa, Journal of Medical Entomology 31 (1994) 333-339.
[13] L. Braack, R. Hunt, L.L. Koekemoer, A. Gericke, G. Munhenga, A.D. Haddow, P. Becker, M. Okia, I. Kimera, M. Coetzee, Biting behaviour of African malaria vectors:1. Where do the main vector species bite on the human body?, Parasites and Vectors 8 (2015).
[14] T.N. Barradas, J.P. Senna, E.R. Júnior, C.R.E. Mansur, Polymer-based drug delivery systems applied to insects repellents devices: A review, Current Drug Delivery 13 (2016) 221-235.
[15] W.W. Focke, W. Van Pareen, Polypropylene-based long-life insecticide-treated mosquito netting, Journal of Polymer Engineering 31 (2011) 521-529.
[16] D.R. Lloyd, K.E. Kinzer, H.S. Tseng, Microporous membrane formation via thermally induced phase separation. I. Solid-liquid phase separation, Journal of Membrane Science 52 (1990) 239-261.
[17] D.R. Lloyd, S.S. Kim, K.E. Kinzer, Microporous membrane formation via thermally-induced phase separation. II. Liquid-liquid phase separation, Journal of Membrane Science 64 (1991) 1-11.
[18] J.W. Cahn, Phase separation by spinodal decomposition in isotropic systems, The Journal of Chemical Physics 42 (1965) 93-99.
[19] J.T. Cabral, J.S. Higgins, Spinodal nanostructures in polymer blends: On the validity of the Cahn-Hilliard length scale prediction, Progress in Polymer Science 81 (2018) 1-21.
[20] M. Liu, S. Liu, Z. Xu, Y. Wei, H. Yang, Formation of microporous polymeric membranes via thermally induced phase separation: A review, Frontiers of Chemical Science and Engineering 10 (2016) 57-75.
[21] C. Sungkapreecha, N. Iqbal, A.M. Gohn, W.W. Focke, R. Androsch, Phase behavior of the polymer/drug system PLA/DEET, Polymer (United Kingdom) 126 (2017) 116-125.
[22] C. Sungkapreecha, M.J. Beily, J. Kressler, W.W. Focke, R. Androsch, Phase behavior of the polymer/drug system PLA/DEET: Effect of PLA molar mass on subambient liquid-liquid phase separation, Thermochimica Acta 660 (2018) 77-81.
[23] M.U. Akhtar, W.W. Focke, Trapping citronellal in a microporous polyethylene matrix, Thermochimica Acta 613 (2015) 61-65.
[24] W.R. Burghardt, Phase diagrams for binary polymer systems exhibiting both crystallization and limited liquid-liquid miscibility, Macromolecules 22 (1989) 2482-2486.
[25] WHO, Guidelines for efficacy testing of mosquito repellents for human skin, World Health Organisation, Geneva, 2009.
[26] D.R. Barnard, R.D. Xue, Laboratory evaluation of mosquito repellents against Aedes albopictus, Culex nigripalpus, and Ochlerotatus triseriatus (Diptera: Culicidae), Journal of Medical Entomology 41 (2004) 726-730.
[27] WHO, Guidelines for efficacy testing of mosquito repellents for human skin, World Health Organization, Geneva, Switzerland, 2009.
[28] M.J. Pascual-Villalobos, A. Robledo, Screening for anti-insect activity in Mediterranean plants, Industrial Crops and Products 8 (1998) 183-194.
[29] J.I. Karr, T.J. Speaker, G.B. Kasting, A novel encapsulation of N,N-diethyl-3-methylbenzamide (DEET) favorably modifies skin absorption while maintaining effective evaporation rates, Journal of Controlled Release 160 (2012) 502-508.

LIST OF FIGURES

**Figure 1.** Schematic phase diagram of a typical miscible polymer-repellent system. The system forms a homogeneous solution above the upper critical solution temperature ($T_{UC}$). The solid line defines the binodal phase boundary and the broken line the spinodal envelope. The arrow indicates the locus of a shock cooling of the homogeneous melt down to a temperature within the spinodal region.

**Figure 2.** A photograph of a footlet prepared for a foot-in-cage test

**Figure 3.** Model of the microporous strand showing the liquid core location, the vapour-filled microporous region and the outer skin layer that functions like a membrane that limits the rate at which the repellent is released.

**Figure 4.** TGA mass loss traces for DEET, neat polymers and (a) LLDPE, and (b) EVA-based strands containing 5 wt-% Dellite 43B clay and either 20 or 30 wt-% DEET.

**Figure 5.** SEM micrographs showing the effect of insect repellent type and concentration on the structure of the internal microporous region of extruded LLDPE strands. (a) 20 wt-% DEET; (b) 30 wt-% DEET; (c) 20 wt-% Icaridin, and (d) 30 wt-% Icaridin. All strands contained 5 wt-% Dellite 43B clay.

**Figure 6.** SEM micrographs obtained after leaching of an LLDPE strand initially containing 30 wt-% DEET and 5 wt-% Dellite 43B clay. (a) Cross-section evidently showing the outer skin covering of the strand; (b) side view of the cut strand; (c) appearance of the microporous

inner surface (imaged after fracture in liquid nitrogen) contrasted with (d) the outer surface appearance of the skin.

**Figure 7.** Repellent release curves during oven ageing at 50 °C. The LLDPE- and EVA-based strands contained 5 wt-% Dellite 43B clay and either DEET or Icaridin as repellent.

**Figure 8.** Bar plot of foot-in-cage repellent test results for polymer strands containing either DEET or Icaridin as repellents. All the compositions utilized Dellite 43B clay as the thickening agent. The strands were aged at 50 °C in a convection oven and the bioassay tests were done every two weeks for up to 12 weeks.

LIST OF TABLES

**Table 1.** Polymer swelling by repellents expressed in wt-% and the permeability of clay-containing blown films in units of $g \cdot \mu m \cdot day^{-1} \cdot m^{-2}$. Both properties were evaluated at 50 °C

**Table 2.** Insect repellent content, strand diameters, release model parameters and estimated membrane thickness for LLDPE and EVA microporous strands.

**Table 3.** Foot-in-cage mosquito repellent test results

**Table 1.** Polymer swelling by repellents expressed in wt-% and the permeability of clay-containing blown films in units of $g \cdot \mu m \cdot day^{-1} \cdot m^{-2}$. Both properties were evaluated at 50 °C

| | DEET | | Icaridin | |
|---|---|---|---|---|
| **Polymer** | **Swelling** | **Permeability** | **Swelling** | **Permeability** |
| LLDPE | 0.78±0.03 | 304±35 | 0.43±0.06 | 135±52 |
| EVA | 5.20±0.11 | 370±33 | 3.14±0.27 | 158±8 |

**Table 2.** Insect repellent content, strand diameters, release model parameters and estimated membrane thickness for LLDPE and EVA microporous strands.

| **Polymer** | **DEET (wt-%)** | **Diameter (mm)** | $\kappa_1 \times 10^3$ **($day^{-1}$)** | $\kappa_2$ **(-)** | $\kappa_3 \times 10^3$ **($day^{-1}$)** | $z_{membrane}$ **(μm)** |
|---|---|---|---|---|---|---|
| LLDPE | 19.30±0.61 | 4.39±0.17 | 1.634 | 1.240 | | 17 |
| LLDPE | 30.03±0.85 | 4.08±0.12 | 2.829 | 1.909 | 2.866 | 20 |
| EVA | 18.72±0.47 | 3.42±0.20 | 6.507 | 1.262 | | 4 |
| EVA | 29.03±0.21 | 3.40±0.16 | 1782 | 208.5 | 8.575 | 8 |
| **Polymer** | **Icaridin (wt-%)** | **Diameter (mm)** | $\kappa_1 \times 10^3$ **($day^{-1}$)** | $\kappa_2$ **(-)** | $\kappa_3 \times 10^3$ **($day^{-1}$)** | $z_{membrane}$ **(μm)** |
| LLDPE | 20.17±0.55 | 2.26±0.05 | 84.73 | 95.95 | - | 40 |
| LLDPE | 29.02±0.22 | 2.15±0.06 | 28.80 | 51.19 | - | 59 |
| EVA | 19.55±0.19 | 4.16±0.21 | 250.0 | 65.97 | 3.844 | 47 |
| EVA | 30.11±0.47 | 2.86±0.18 | 1476 | 318.6 | 4.646 | 26 |

**Table 3.** Foot-in-cage mosquito repellent test results

| | | | | | | | # of bites on foot | | |
|---|---|---|---|---|---|---|---|---|---|
| **Polymer** | **Repellent** | **Level wt-%** | **Ageing weeks** | **Test person** | **Foot (L/R)** | **1st bite s** | **Untreated #** | **Treated #** | **Protection %** |
| LLDPE | DEET | 20 | 1 | X | R | 10 | 49 | 6 | 78 |
| LLDPE | DEET | 20 | 3 | Z | L | 23 | 39 | 4 | 81 |
| LLDPE | DEET | 20 | 5 | Z | L | 48 | 16 | 0 | 100 |
| LLDPE | DEET | 20 | 7 | Z | R | 103 | 20 | 6 | 54 |
| LLDPE | DEET | 20 | 9 | Y | R | 30 | 11 | 0 | 100 |
| LLDPE | DEET | 20 | 11 | Y | L | 54 | 26 | 6 | 63 |
| LLDPE | DEET | 30 | 1 | Z | R | 20 | 26 | 8 | 53 |
| LLDPE | DEET | 30 | 3 | Z | R | 21 | 98 | 12 | 78 |
| LLDPE | DEET | 30 | 5 | X | R | 62 | 7 | 0 | 100 |
| LLDPE | DEET | 30 | 7 | X | R | 79 | 40 | 1 | 95 |
| LLDPE | DEET | 30 | 9 | Y | R | 27 | 7 | 2 | 56 |
| LLDPE | DEET | 30 | 11 | X | L | 26 | 47 | 4 | 84 |
| LLDPE | Icaridin | 20 | 1 | Z | L | 13 | 47 | 1 | 96 |
| LLDPE | Icaridin | 20 | 3 | X | R | 10 | 24 | 3 | 78 |
| LLDPE | Icaridin | 20 | 5 | X | L | 51 | 45 | 0 | 100 |
| LLDPE | Icaridin | 20 | 7 | Z | R | 35 | 18 | 1 | 89 |
| LLDPE | Icaridin | 20 | 9 | X | R | 27 | 27 | 6 | 64 |
| LLDPE | Icaridin | 20 | 11 | X | L | 43 | 41 | 15 | 46 |
| LLDPE | Icaridin | 30 | 1 | X | L | 105 | 18 | 1 | 89 |
| LLDPE | Icaridin | 30 | 3 | X | L | 15 | 62 | 0 | 100 |
| LLDPE | Icaridin | 30 | 5 | Z | L | 29 | 24 | 0 | 100 |
| LLDPE | Icaridin | 30 | 7 | Z | L | 57 | 20 | 0 | 100 |
| LLDPE | Icaridin | 30 | 9 | X | L | 24 | 7 | 0 | 100 |
| LLDPE | Icaridin | 30 | 11 | Y | L | 54 | 48 | 1 | 96 |

| | | | | | | | | | |
|---|---|---|---|---|---|---|---|---|---|
| EVA | DEET | 20 | 2 | Z | R | 45 | 36 | 0 | 100 |
| EVA | DEET | 20 | 4 | X | R | 50 | 33 | 0 | 100 |
| EVA | DEET | 20 | 6 | X | L | 32 | 11 | 0 | 100 |
| EVA | DEET | 20 | 8 | Z | L | 115 | 65 | 13 | 67 |
| EVA | DEET | 20 | 10 | X | L | 57 | 28 | 8 | 56 |
| EVA | DEET | 20 | 12 | X | R | 21 | 29 | 2 | 87 |
| EVA | DEET | 30 | 2 | X | L | 25 | 21 | 0 | 100 |
| EVA | DEET | 30 | 4 | Z | R | 36 | 17 | 0 | 100 |
| EVA | DEET | 30 | 6 | Z | L | 25 | 11 | 1 | 83 |
| EVA | DEET | 30 | 8 | X | R | 90 | 20 | 1 | 90 |
| EVA | DEET | 30 | 10 | Y | L | 75 | 43 | 16 | 46 |
| EVA | DEET | 30 | 12 | Y | R | 13 | 55 | 8 | 75 |
| EVA | Icaridin | 20 | 2 | Z | L | 20 | 22 | 0 | 100 |
| EVA | Icaridin | 20 | 4 | Z | L | 115 | 7 | 1 | 75 |
| EVA | Icaridin | 20 | 6 | Z | R | 34 | 78 | 4 | 90 |
| EVA | Icaridin | 20 | 8 | Z | L | 28 | 24 | 0 | 100 |
| EVA | Icaridin | 20 | 10 | Y | R | 29 | 13 | 0 | 100 |
| EVA | Icaridin | 20 | 12 | Y | L | 6 | 62 | 6 | 82 |
| EVA | Icaridin | 30 | 2 | X | L | 40 | 23 | 0 | 100 |
| EVA | Icaridin | 30 | 4 | X | L | 170 | 7 | 0 | 100 |
| EVA | Icaridin | 30 | 6 | X | R | 40 | 57 | 3 | 90 |
| EVA | Icaridin | 30 | 8 | X | R | 51 | 50 | 0 | 100 |
| EVA | Icaridin | 30 | 10 | X | R | - | 24 | 5 | 66 |
| EVA | Icaridin | 30 | 12 | X | L | 6 | 71 | 12 | 71 |

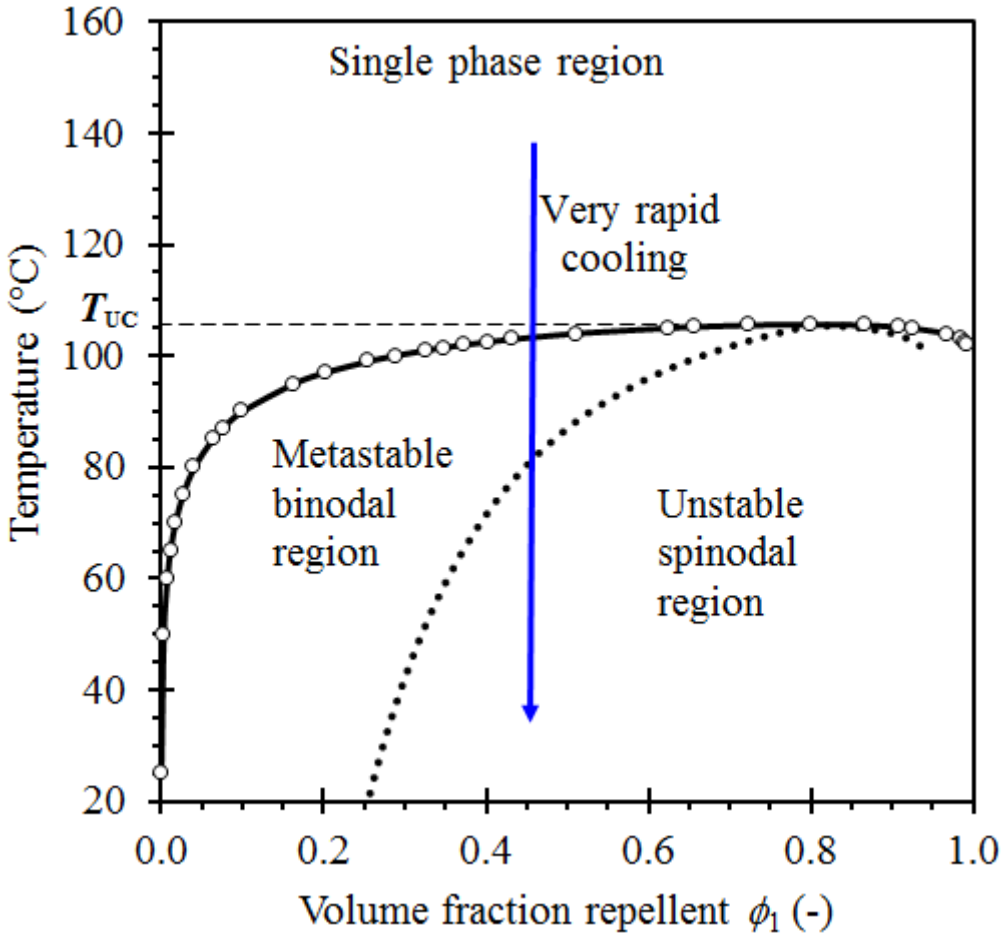


**Figure 1.** Schematic phase diagram of a typical miscible polymer-repellent system. The system forms a homogeneous solution above the upper critical solution temperature ($T_{UC}$). The solid line defines the binodal phase boundary and the broken line the spinodal envelope. The arrow indicates the locus of a shock cooling of the homogeneous melt down to a temperature within the spinodal region.

**Figure 2.** A photograph of a footlet prepared for a foot-in-cage test

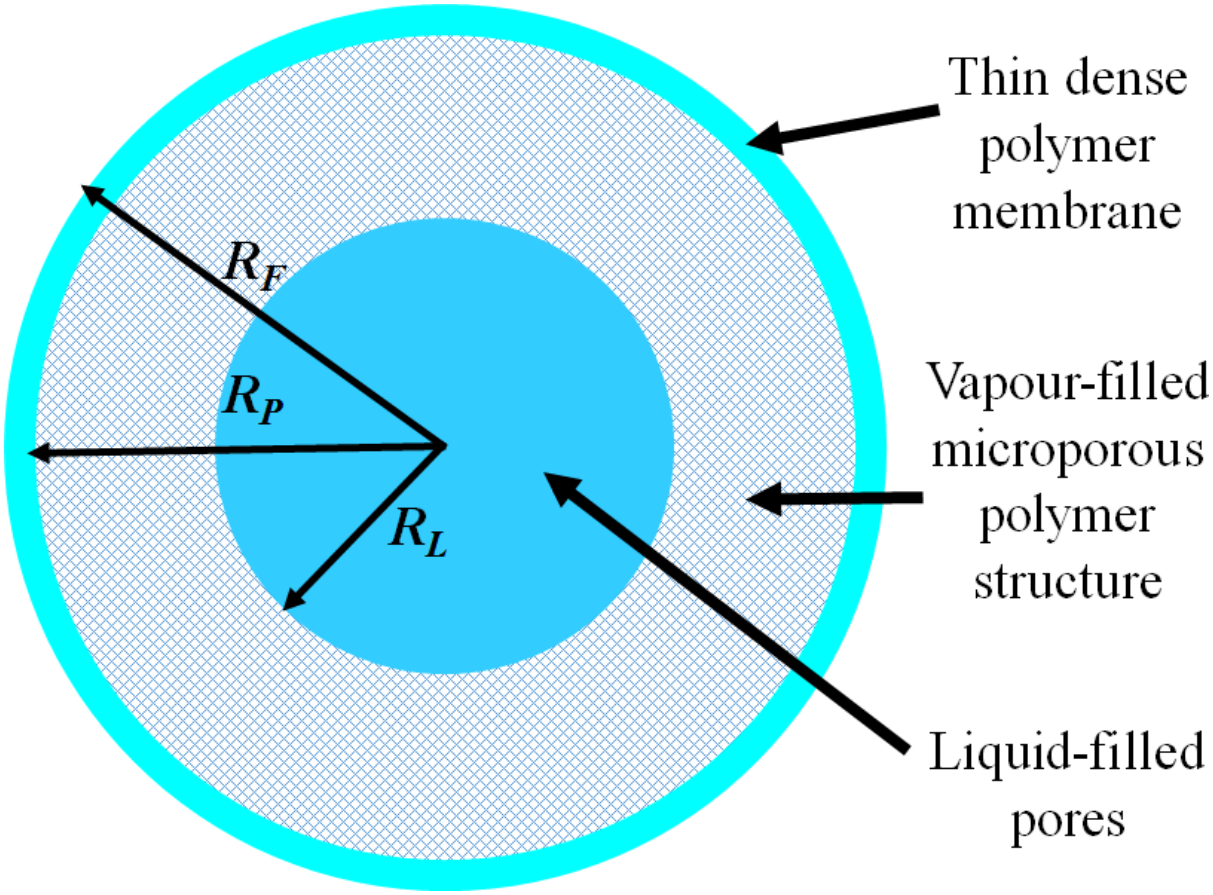


**Figure 3.** Model of the microporous strand showing the liquid core location, the vapour-filled microporous region and the outer skin layer that functions like a membrane that limits the rate at which the repellent is released.

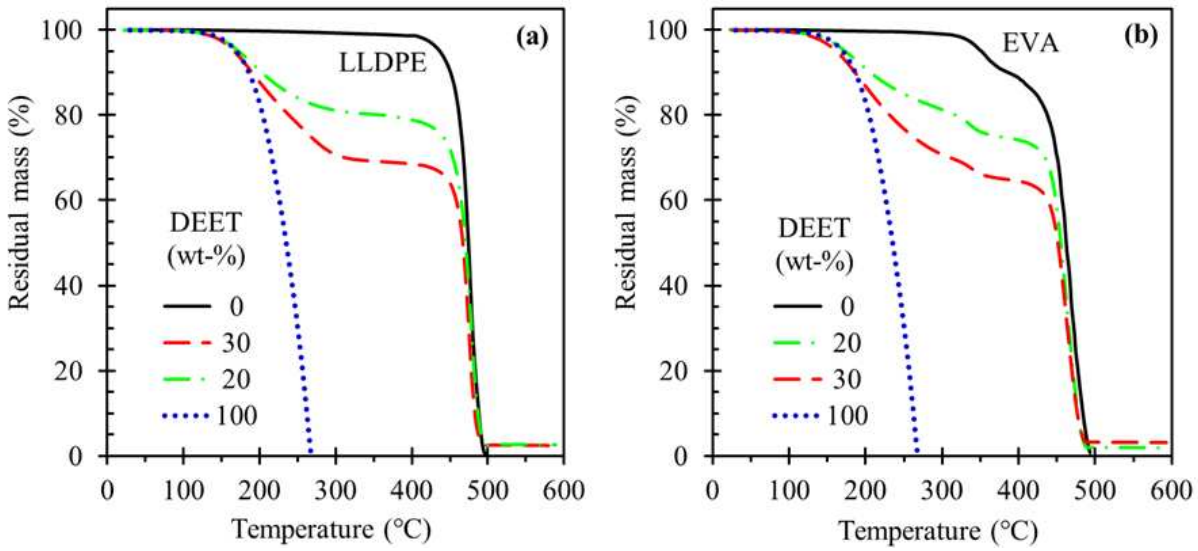


**Figure 4.** TGA mass loss traces for DEET, neat polymers and (a) LLDPE, and (b) EVA-based strands containing 5 wt-% Dellite 43B clay and either 20 or 30 wt-% DEET.

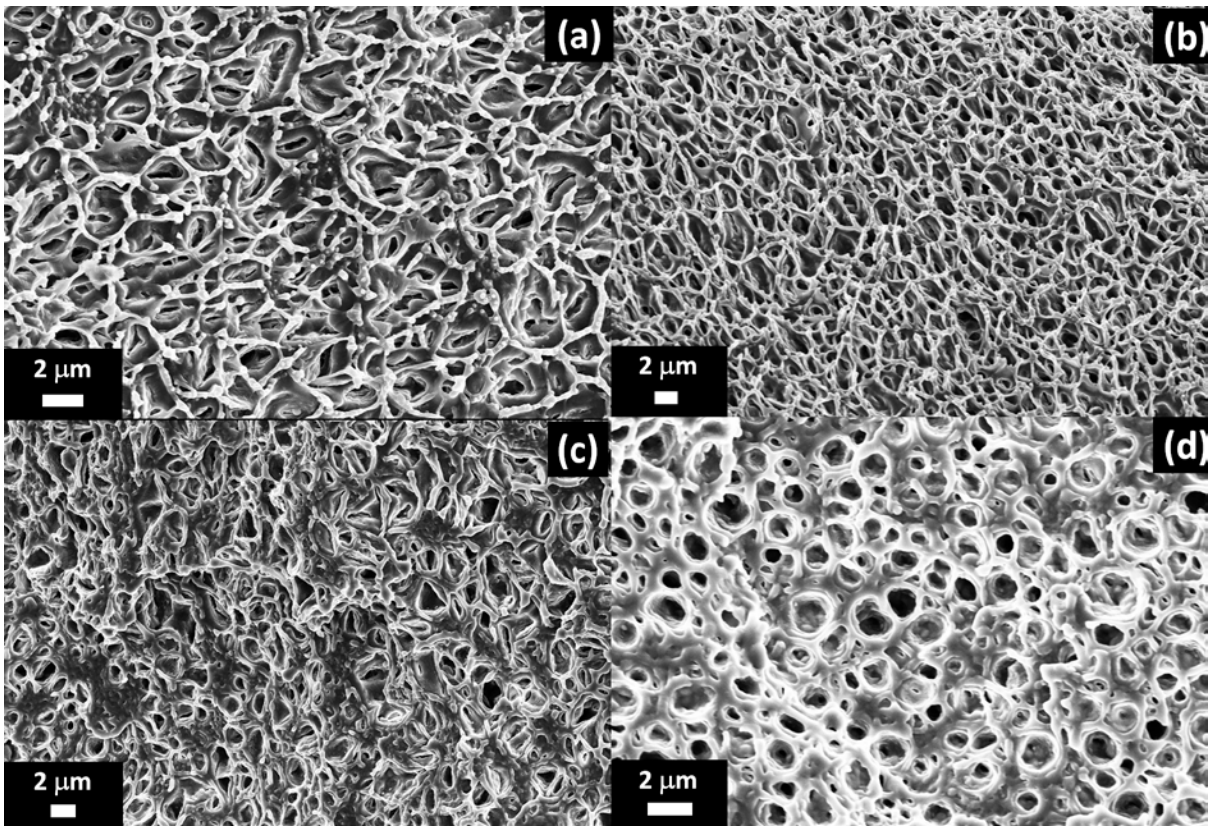


**Figure 5.** SEM micrographs showing the effect of insect repellent type and concentration on the structure of the internal microporous region of extruded LLDPE strands. (a) 20 wt-% DEET; (b) 30 wt-% DEET; (c) 20 wt-% Icaridin, and (d) 30 wt-% Icaridin. All strands contained 5 wt-% Dellite 43B clay.

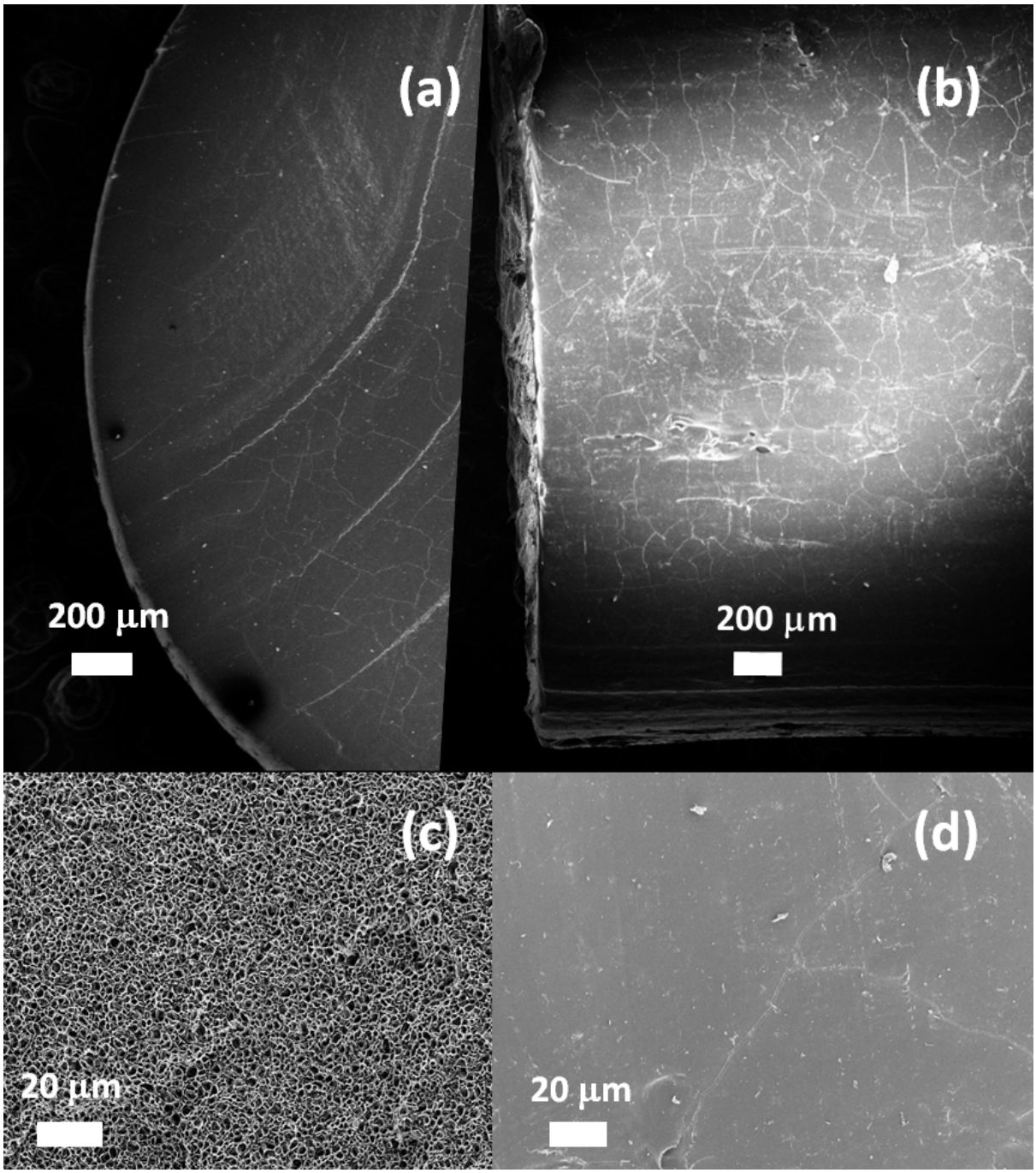


**Figure 6.** SEM micrographs obtained after leaching of an LLDPE strand initially containing 30 wt-% DEET and 5 wt-% Dellite 43B clay. (a) Cross-section evidently showing the outer skin covering of the strand; (b) side view of the cut strand; (c) appearance of the microporous inner surface (imaged after fracture in liquid nitrogen) contrasted with (d) the outer surface appearance of the skin.

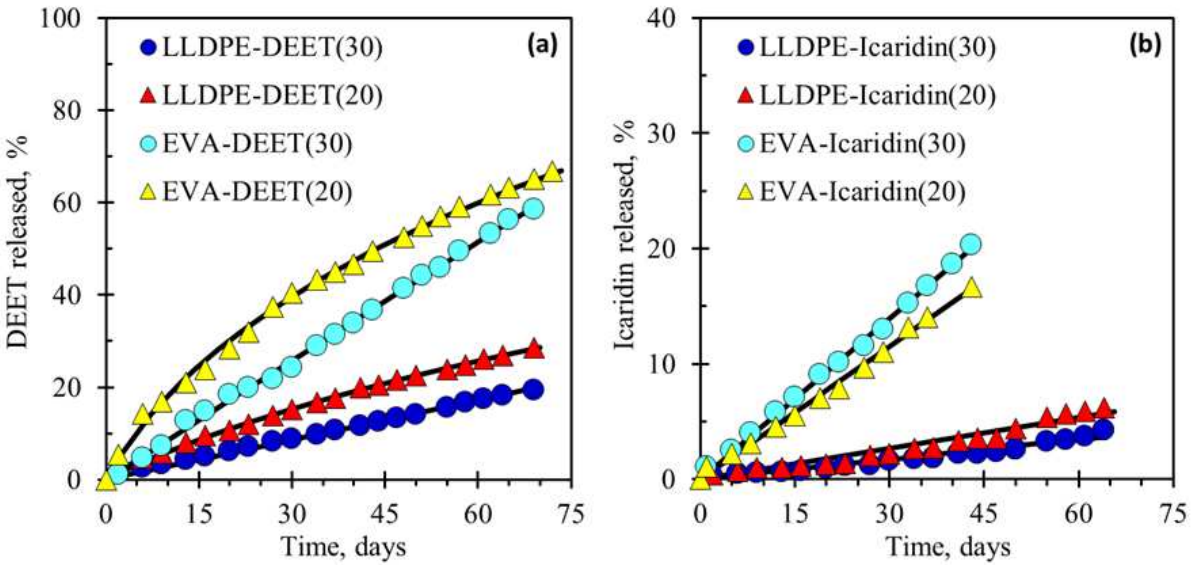


**Figure 7.** Repellent release curves during oven ageing at 50 °C. The LLDPE- and EVA-based strands contained 5 wt-% Dellite 43B clay and either DEET or Icaridin as repellent.

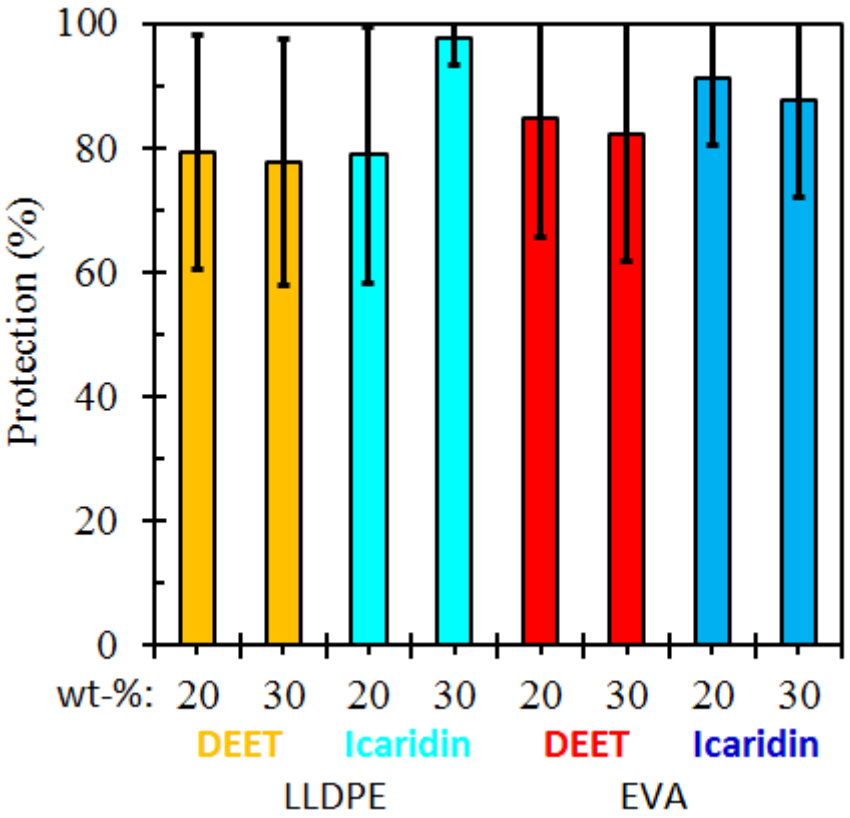


**Figure 8.** Bar plot of foot-in-cage repellent test results for polymer strands containing either DEET or Icaridin as repellents. All the compositions utilized Dellite 43B clay as the thickening agent. The strands were aged at 50 °C in a convection oven and the bioassay tests were done every two weeks for up to 12 weeks.